



CHORUS

This is the accepted manuscript made available via CHORUS. The article has been published as:

Vorticity in electron beams: Definition, properties, and its relationship with magnetism

Ján Ruzs, Juan-Carlos Idrobo, and Linus Wrang

Phys. Rev. B **94**, 144430 — Published 24 October 2016

DOI: [10.1103/PhysRevB.94.144430](https://doi.org/10.1103/PhysRevB.94.144430)

Vorticity in electron beams: Definition, properties, and its relationship with magnetism

Ján Ruzs,¹ Juan-Carlos Idrobo,² and Linus Wrang¹

¹*Department of Physics and Astronomy, Uppsala University, P.O. Box 516, 75120 Uppsala, Sweden**

²*Center of Nanophase Materials Sciences, Oak Ridge National Laboratory, Oak Ridge, TN 37831, USA†*

Vorticity is a concept well established in fluid dynamics to describe the local tendency of a fluid to rotate. Here, we explore the vorticity of electron waves, and show that it can be used to qualitatively estimate the strength of an electron magnetic circular dichroism (EMCD) signal, without resorting in expensive inelastic electron scattering calculations. We discuss the properties of vorticity, its relationship with orbital angular momentum and how it can be used to investigate the characteristics of electron beams.

PACS numbers: 61.05.J-, 41.20.Jb, 41.85.-p, 42.50.Tx

Keywords: vorticity, electron beam, aberrations, magnetic circular dichroism

Electron magnetic circular dichroism (EMCD) is a young experimental method for measuring magnetic properties at high spatial resolution in [scanning] transmission electron microscopy (S/TEM). During its decade of existence since the first experimental confirmation¹, EMCD has gone through a rapid development. In principle, EMCD experiments should be able to achieve the ultimate spatial resolution, allowing magnetic characterization of individual magnetic atomic columns. Electron vortex beams (EVBs;²⁻⁵) and aberrated beams^{6,7} of atomic size are both expected to be efficient probes of magnetism. Initial experiments aiming to detect EMCD with atomic size probes have been reported with aberrated beams⁸. However, as of today, these experiments remain challenging to perform. Understanding how different kind of electron beams can be optimized to measure not only magnetism, but also different chiral signals is crucial for future successful experiments.

In this Letter, we study the properties of electron beams via the introduction of vorticity. We show that vorticity is a local measure of orbital angular momentum (OAM). We show that aberrated beams can be understood as a coherent superposition of an Airy disk and rings of electron vortices. We also show that the strength of EMCD can be well estimated by the vorticity of electron beams, which is accessible from computationally-inexpensive elastic electron scattering calculations.

Vorticity⁹, which is a concept well established in fluid mechanics, is used to describe the local tendency of a fluid to rotate. Vorticity is widely applied to study the dynamics of turbulent fluids covering fields that go from chemical engineering, mechanical and aeronautical engineering, to atmospheric, oceanographic and planetary sciences¹⁰. Vorticity is defined as $\Theta = \nabla \times \mathbf{u}$, with \mathbf{u} being the velocity of the fluid.

Here, we explore the concept of vorticity for waves generated by electron beams. For an electron wave, the velocity is represented by the probability current $\mathbf{j} = \frac{\hbar}{m_e} \text{Im}[\psi^* \nabla \psi]$ ¹², where \hbar is the reduced Planck constant, ψ is the wave function associated to the electron beam, and m_e is the mass of the electron. As such, the

vorticity for an electron wave is simply defined as¹¹

$$\Theta = \frac{\hbar}{m_e} \nabla \times \text{Im}[\psi^* \nabla \psi] = -\frac{i\hbar}{m_e} \nabla \psi^* \times \nabla \psi. \quad (1)$$

To conceptually illustrate how the vorticity Θ can be utilized to capture the behavior of electrons, we explicitly calculate Θ for different kind of electron beams. The first example is vortex beams, which can be produced by hologram grids inside of an electron microscope³⁻⁵. Vortex beams have a doughnut-like intensity profile and carry OAM as it is shown in Figure 1. A vortex beam within an electron microscope can be expressed in cylindrical coordinates as

$$\psi_l(r, \varphi, z) = e^{il\varphi} R_l(r, z), \quad (2)$$

where $l\hbar$ is the value of OAM carried by the vortex beam, and R_l is a function that describes the amplitude behavior of the vortex. R_l depends on the optical parameters of the electron microscope, such as the convergence objective angle θ_c , defocus ($\Delta f = z$), and the wavelength of the electron λ – which is determined by the applied acceleration voltage. [For a round aperture and flat amplitude distribution](#) the radial dependence of a vortex beam is

$$R_l = \int_0^{\theta_c} e^{i\frac{\pi}{\lambda} \Delta f \theta^2} J_l\left(\frac{2\pi}{\lambda} \theta r\right) \theta d\theta, \quad (3)$$

where J_l is the Bessel function of the first kind with order l ¹³. Notice that for the case of $l = 0$, Eqns. 2 and 3 lead to an [Airy-disc](#)¹⁴. [Airy disc wavefunction describes](#) the behavior of electron beams in an electron microscope column under the absence of aberrations. ([It is not to be confused with Airy waves](#)¹⁵.)

The vorticity of a vortex beam utilizing the definition shown in Eq. 2 is

$$\begin{aligned} \Theta_r &= l \frac{\hbar}{m_e r} (R_l \partial_z R_l^* + R_l^* \partial_z R_l), \\ \Theta_\varphi &= i \frac{\hbar}{m_e} (\partial_r R_l^* \partial_z R_l - \partial_r R_l \partial_z R_l^*), \\ \Theta_z &= l \frac{\hbar}{m_e r} (R_l \partial_r R_l^* + R_l^* \partial_r R_l). \end{aligned} \quad (4)$$

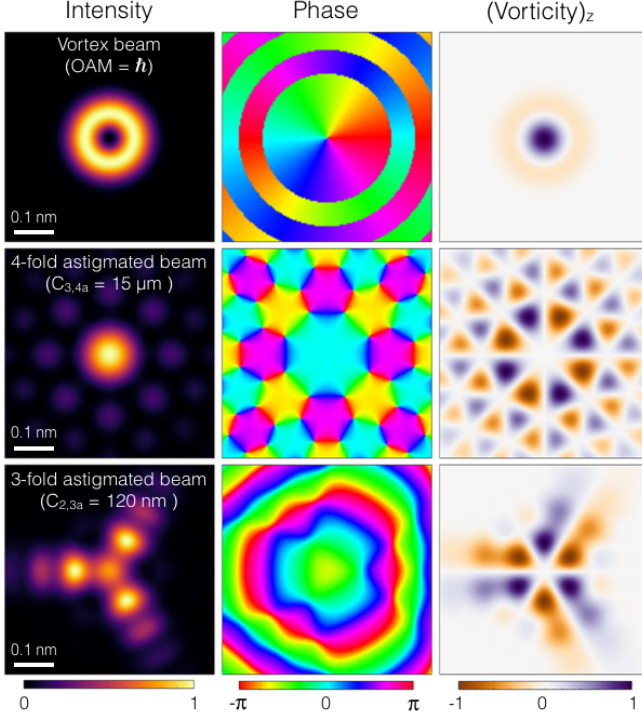


FIG. 1. Normalized wavefunctions and normalized vorticities of an electron vortex beam, a four-fold astigmatic beam, and a three-fold astigmatic beam. The calculations were performed using an acceleration voltage of 100 kV and a convergence semi-angle $\alpha = 30$ mrad. The spatial range of all panels is $0.5 \text{ nm} \times 0.5 \text{ nm}$. All the panels for the vortex and four-fold astigmatic beams are shown for a defocus value $\Delta f = 0 \text{ nm}$, while for the three-fold astigmatic beam $\Delta f = -0.6 \text{ nm}$.

Few conclusions can easily be drawn from a simple inspection of Eq. 4. The r and z components of the vorticity are zero for an Airy disk electron beam, i.e., $l = 0$. This means that the vorticities Θ_r and Θ_z of an aberration-corrected electron probe are always zero. For the case of a vortex beam with OAM $l\hbar$, the vorticity Θ_z reaches its maximum value at zero defocus ($\Delta f = z = 0$), and this value is proportional to $2R_l \partial_r R_l$ - i.e., $R_l^* = R_l$ at $z = 0$. Conversely, the vorticity Θ_φ component is different than zero at $\Delta f = 0$, with a magnitude that is proportional to $\partial_r R_l \partial_z R_l$ for all l s. For different defocus values, Θ_φ is also different than zero for all l s, indicating that **the azimuthal component of the vorticity is always nonzero**.

As it will be shown below, the concept of vorticity becomes rather useful and insightful when working with aberrated electron beams. Here we will only illustrate the case of vorticity for electron beams containing a single no cylindrical symmetry aberration (i.e., beam shift, two fold astigmatism, coma, three fold astigmatism, four fold astigmatism, etc.). Krivanek's notation is used here to label the aberrations because it simplifies the mathematical description for all kind of aberrations¹⁶.

The angular dependence of an aberration $C_{n,m}$ of or-

der n and multiplicity m (or symmetry) is given by $\frac{2\pi}{\lambda} \frac{\theta^{n+1}}{n+1} \cos(m\varphi)$ for mirror-symmetric aberrations (labeled as $C_{n,m,a}$), and $\frac{2\pi}{\lambda} \frac{\theta^{n+1}}{n+1} \sin(m\varphi)$ for antisymmetric aberrations (labeled as $C_{n,m,b}$).

It can be shown that the wave function of a mirror-symmetric aberrated beam $\psi_{n,m}$ can be expressed as (see Appendix A for details)

$$\psi_{n,m} = 2\pi R_0 + \sum_{l=1}^{\infty} A_{l,m} P_{l,n,m} (e^{ilm\varphi} + e^{-ilm\varphi}), \quad (5)$$

where R_0 is defined in Eq. 3 for $l = 0$, $A_{l,m} = 2\pi i^{l(m+1)}$ is a phase coefficient, and $P_{l,n,m}$ is

$$\int_0^{\theta_c} e^{i\frac{\pi}{\lambda}\Delta f\theta^2} J_{lm} \left(\frac{2\pi}{\lambda}\theta r \right) J_l \left(\frac{2\pi}{\lambda(n+1)}\theta^{n+1} C_{n,m,a} \right) \theta d\theta. \quad (6)$$

Notice that $\psi_{n,m}$ is a sum of an Airy disk wave plus the sum of interfering vortex beams with opposite OAM ($\pm lm\hbar$). In other words, vortex beams created entirely by means of an aberrated lens are not intrinsically separated in space, since all the vortex beams and the Airy disk wave produced by an aberrated lens are centered around $r = 0$. However, since the aberrated beam $\psi_{n,m}$ is the result of a coherent interference of vortex beams, there must be local regions where the vortices cancel each other out, and regions where they do not cancel out and possibly create a new vortex. It is here where the concept of vorticity brings new light into the properties of aberrated beams, and how they can be utilized to do novel spectroscopy.

In principle, aberrated beams, similarly as vortex beams, should have a vorticity that is far more complex than Airy disk waves. However, that is not always the case. For instance, an aberrated beam with an odd aberration multiplicity (i.e., beam shift, coma, or three fold astigmatism) presents a simpler vorticity behavior than an aberrated beam with even multiplicity. Similarly to Airy disk waves, it can be shown that aberrated beams with odd multiplicity have **a vorticity Θ_z component that is zero**, but only for $\Delta f = 0$. Aberrated beams with even multiplicity have **a vorticity Θ_z that is different than zero** at $\Delta f = 0$. Also both multiplicities, odd and even, result in aberrated beams with a vorticity Θ_φ that is not zero for any value of z .

Figure 1 shows the electron probe intensity, phase and vorticity Θ_z calculated for a vortex beam with \hbar OAM, and aberrated electron beams with four fold astigmatism ($C_{3,4,a} = 15 \mu\text{m}$), and three fold astigmatism ($C_{2,3,a} = 120 \text{ nm}$). Notice that the maximum values of the z component of the vorticity for **a vortex beam and a four-fold astigmatic probe occurs near** the center of a region where a phase singularity is present (defined as a circular-like phase ramping with null intensity). In a vortex beam this occurs at $r = 0$. Conversely, for **a four-fold astigmatic beam the phase singularities occur at the tails** of the beam, in between regions where the amplitude of

the tails presents a local maxima. In general, however, one can find maxima of vorticity without phase singularities in the electron beam wavefunction. This can be seen in a three-fold astigmatic probe with defocus, Fig. 1.

Intuitively it may appear that the vorticity $\Theta(\mathbf{r})$ and the OAM density, defined as $\psi^*(\mathbf{r})\hat{\mathbf{L}}\psi(\mathbf{r}) = m_e\mathbf{r} \times \mathbf{j}$ (where $\hat{\mathbf{L}}$ is the angular momentum operator), should be closely related to each other. It was even suggested in Ref. 17 that for a vortex beam, vorticity and OAM density are proportional to each other. Clearly, the planar integral of the z component of the OAM density results in the total OAM of the beam. However, the integral of the vorticity can conveniently be re-expressed using the momentum operator $\hat{\mathbf{p}}$ as $\frac{i}{m_e\hbar}\langle\psi|\hat{\mathbf{p}}\times\hat{\mathbf{p}}|\psi\rangle$. Then it becomes obvious that the total vorticity is simply zero. Therefore the relation between OAM density and vorticity is more subtle.

To derive the relationship between OAM density and vorticity, only the z component of the OAM density is considered here. The OAM density centered around point \mathbf{a} is $L_{\mathbf{a}}(\mathbf{r}) = m_e(\mathbf{r} - \mathbf{a}) \times \mathbf{j}(\mathbf{r})$. Taylor-expanding the L_z component around a point \mathbf{a} , and integrating only in the xy plane over a small circle D centered around \mathbf{a} , the zero order term vanishes due to $(\mathbf{r} - \mathbf{a})$ factor evaluated at $\mathbf{r} = \mathbf{a}$. The linear terms vanish as well, because they are odd functions integrated over a symmetric region D . The lowest order nonzero terms are the second order terms, except for the mixed (x, y) term, which vanishes for the same reason as the linear terms. This results in the following approximation:

$$\int_D dx dy L_{z,\mathbf{a}} \approx \frac{1}{2} \int_D dx dy \left[(x - a_x)^2 \frac{\partial^2 L_{z,\mathbf{a}}}{\partial x^2} \Big|_{\mathbf{a}} + (y - a_y)^2 \frac{\partial^2 L_{z,\mathbf{a}}}{\partial y^2} \Big|_{\mathbf{a}} \right]. \quad (7)$$

In the next step one realizes that

$$\int_D dx dy (x - a_x)^2 \frac{\partial^2 L_{z,\mathbf{a}}}{\partial x^2} \Big|_{\mathbf{a}} = m_e \frac{\partial j_y}{\partial x} \Big|_{\mathbf{a}} \int_D dx dy (x - a_x)^2, \quad (8)$$

and similarly for the term with the y derivative. Thus one finally obtains

$$\int_D dx dy L_{z,\mathbf{a}} \propto m_e \left[\frac{\partial j_y}{\partial x} \Big|_{\mathbf{a}} - \frac{\partial j_x}{\partial y} \Big|_{\mathbf{a}} \right] = m_e \Theta_z(\mathbf{a}), \quad (9)$$

which means that the vorticity can be interpreted as a local measurement of OAM. Fig. 1 showing the z component of the vorticity for a four-fold astigmatic beam suggests that it can be qualitatively understood as a superposition of an Airy disk in the center with surrounding rings of electron vortices with alternating OAM¹⁸.

Next, we proceed with the derivation of a more unexpected relationship, namely the connection between vorticity and EMCD.

To derive the relation between vorticity and EMCD, we need to start from the expression that describes elec-

tron inelastic scattering events in STEM, i.e., the double-differential scattering cross-section (DDSCS)

$$\frac{\partial^2 \sigma}{\partial \Omega \partial E} \propto \sum_{I,F} \left| \langle \psi_f | \otimes \langle F | \hat{V} | I \rangle \otimes | \psi_i \rangle \right|^2 \delta(E_F - E_I - E), \quad (10)$$

where $|I\rangle, |F\rangle$ are the initial and final state of the sample with energies E_I, E_F , respectively, and $|\psi_i\rangle, |\psi_f\rangle$ are the electron probe states before and after a core-level excitation event. The electron probe is expressed before the inelastic scattering event using its Fourier transform as $\psi_i(\mathbf{r}) = \int C(\mathbf{k}) e^{i\mathbf{k}\cdot\mathbf{r}} d\mathbf{k}$. Elastic scattering is neglected after the excitation event by writing $\psi_f(\mathbf{r}) = e^{i\mathbf{k}_f\cdot\mathbf{r}}$. Finally, the mixed-dynamical form factor (MDFF) is written in the dipole approximation. The imaginary part of MDFF, which is responsible for a magnetic signal in electron energy-loss spectroscopy (EELS)^{1,7}, is $\text{Im}[S_{\mathbf{a}}(\mathbf{q}, \mathbf{q}', E)] \propto (\mathbf{q} \times \mathbf{q}') \cdot \mathbf{M}(E)$, where $\mathbf{M}(E)$ is an energy-loss dependent vector characterizing the magnetic behavior of a specific material. Thus, the magnetic part of the DDSCS can be written as

$$\frac{\partial^2 \sigma}{\partial \Omega \partial E} \Big|_{\text{mag}} \propto \sum_{\mathbf{a}} \iiint d\mathbf{r} d\mathbf{r}' d\mathbf{k} d\mathbf{k}' \psi_i(\mathbf{r}) e^{-i\mathbf{k}\cdot\mathbf{r}} \psi^*(\mathbf{r}') e^{i\mathbf{k}'\cdot\mathbf{r}'} \times e^{i(\mathbf{k}-\mathbf{k}')\cdot\mathbf{a}} \frac{i(\mathbf{k}_f - \mathbf{k}) \times (\mathbf{k}_f - \mathbf{k}')}{(\mathbf{k}_f - \mathbf{k})^2 (\mathbf{k}_f - \mathbf{k}')^2} \cdot \mathbf{M}(E) \quad (11)$$

where $\mathbf{q} = \mathbf{k}_f - \mathbf{k}$. $C(\mathbf{k})$ has been substituted for $\int \psi_i(\mathbf{r}) e^{-i\mathbf{k}\cdot\mathbf{r}} d\mathbf{r}$, and similarly for primed variables $\mathbf{q}', C(\mathbf{k}')$. Sum over \mathbf{a} runs over all atomic positions, where an excitation event can take place. For convergent probes, such as in STEM, that vanish in infinity, one can use the relation

$$\int i\mathbf{k}\psi_i(\mathbf{r}) e^{i\mathbf{k}\cdot\mathbf{r}} d\mathbf{r} = \int \nabla\psi_i(\mathbf{r}) e^{i\mathbf{k}\cdot\mathbf{r}} d\mathbf{r} \quad (12)$$

for derivatives of Fourier transforms. In the next steps we analytically integrate over \mathbf{k}, \mathbf{k}' and use the Ansatz $\psi_i(\mathbf{r}) = e^{i\mathbf{k}_i\cdot\mathbf{r}} \phi_i(\mathbf{r})$ commonly used in multislice methods, expressing electron beam wavefunction as a product of plane wave times a smoothly varying envelope function $\phi_i(\mathbf{r})$. For a symmetrical on-axis detector and $\mathbf{M}(E) \parallel \mathbf{k}_i$ we finally arrive to an expression for the magnetic part of the inelastic scattering cross-section (see Appendix B for a detailed derivation)

$$\frac{\partial \sigma}{\partial E} \Big|_{\text{mag}} \propto \sum_{\mathbf{a}} \int_{\Omega} d\mathbf{k}_{f,\perp} \iint d\mathbf{r} d\mathbf{r}' \frac{e^{-i(\mathbf{k}_f - \mathbf{k}_i) \cdot (\mathbf{r} - \mathbf{r}')}}{|\mathbf{r} - \mathbf{a}| |\mathbf{r}' - \mathbf{a}|} \times i\mathbf{M}(E) \cdot [\nabla\phi_i(\mathbf{r}) \times \nabla'\phi_i^*(\mathbf{r}')], \quad (13)$$

where the integral over $\mathbf{k}_{f,\perp}$ runs over any circular or annular detector aperture centered on axis. The second line of this expression reminds vorticity, however it is evaluated at two different positions \mathbf{r}, \mathbf{r}' . The gradient with prime, ∇' , means a gradient with respect to the primed coordinate \mathbf{r}' . The weight of contributions from \mathbf{r}, \mathbf{r}' is given by the first line and the largest contributions

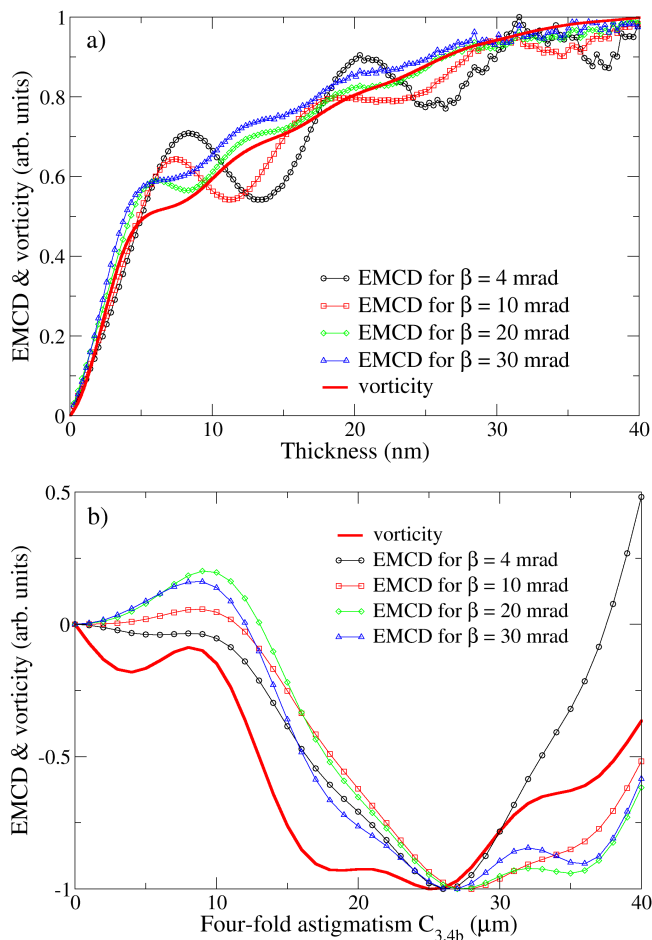


FIG. 2. a) Thickness dependence of the EMCD compared with the sum of vorticity over atomic positions, $\sum_{\mathbf{a}} \Theta_z(\mathbf{a})$. Calculations were performed for an EVB with $\text{OAM}=\hbar$, convergence semi-angle $\alpha = 27.5$ mrad and a range of collection semi-angles β indicated in the legend. Sample is bcc iron oriented in (001) zone axis, acceleration voltage is 200 kV. b) Comparison of EMCD and vorticity, $\sum_{\mathbf{a}} \Theta_z(\mathbf{a})$, as a function of strength of four-fold astigmatism $C_{3,4b}$ for an electron beam with convergence angle 30 mrad and acceleration voltage 100 kV.

obviously come from the closest surrounding of positions $\mathbf{r} = \mathbf{r}' = \mathbf{a}$.

Therefore we propose that the strength of EMCD signal can be qualitatively estimated by summing the z -component of the vorticity at the atomic sites. This theorem constitutes the central result of this Letter.

A simple test of its accuracy is shown in Fig. 2(a), where a simulated thickness dependence of the EMCD strength¹⁹ is compared to the sum of z -component of vorticities evaluated at the atomic sites, $\sum_{\mathbf{a}} \Theta_z(\mathbf{a})$. Double-channeling effects are more pronounced at smaller collection angles, which results in an oscillation of the EMCD signal and in a weaker agreement with the calculated vorticity. For larger collection angles the qualitative match between EMCD and vorticity is quite remarkable. This

result is important because it means that when using relatively large collection angles, as in modern STEM experiments (> 20 mrad), vorticity can give a very good qualitative picture of the strength of an EMCD signal. The calculation of vorticity is computationally very cheap (seconds or minutes on a modern personal computer), while an explicit evaluation of the EMCD signal (Eq. 13) can take several days and typically requires a computer cluster.

Similar interpretation can be extracted from Fig. 2(b), where the EMCD strength is compared to the z -component of vorticity summed over atoms, as a function of four-fold astigmatism. Here, a sample thickness of one unit cell is assumed in order to minimize the distortion effects in the electron probe, which are due to elastic scattering. The agreement between the vorticity and EMCD with four-fold astigmatism is weaker than in the previous case. However, the oscillation periods and position of the optimum EMCD signal correlate rather well with the vorticity. Generally, a weaker correspondence of the vorticity and EMCD signal is likely due to a varying delocalization of the vorticity peaks for aberrated probes as a function of the four fold astigmatism, $C_{3,4b}$.

We note that EMCD and vorticity are shown in arbitrary units in Fig. 2. Absolute values would only have sense in a suitably chosen normalization, e.g., relative to the incoming beam intensity. However, as long as the normalization does not change across the range of shown parameters, such as thickness or aberration values, vorticity offers an efficient way to optimize the beam parameters, as well as to analyze thickness-dependence of EMCD. Yet, to provide an approximate scale, the relative strengths of EMCD shown in panels a) and b) reach at maximum about 20% and 5%, respectively. These values are typically only reached for small collection angles, and for vortex beams only at very low sample thicknesses.

In conclusion, we have derived a relation between the vorticity of electron beams, the orbital angular momentum density and the strength of an EMCD signal. Using the concept of vorticity, we also show that aberrated electron beams are composed by a linear combination of vortex beams and an Airy disk that coherently interfere when the aberrations are not cylindrical symmetric. This means that although aberrated beams have a total OAM of zero, locally they contain vortices that can be utilized to measure chiral signals. We also show that vorticity is a computationally efficient alternative to qualitatively estimate the strength of an EMCD signal. The results presented here raise the concept of vorticity to the level of a central property of electron beams that needs to be further investigated.

ACKNOWLEDGMENTS

J.R. acknowledges Swedish Research Council and Swedish National Infrastructure for Computing (NSC

center). J.-C.I. acknowledges support by the Center for Nanophase Materials Sciences (CNMS), which is spon-

sored at Oak Ridge National Laboratory by the Scientific User Facilities Division, Office of Basic Energy Sciences, U.S. Department of Energy.

* jan.rusz@physics.uu.se

† idrobojc@ornl.gov

- ¹ P. Schattschneider, S. Rubino, C. Hébert, J. Rusz, J. Kuneš, P. Novák, E. Carlino, M. Fabrizio, G. Panaccione and G. Rossi, *Nature* **441**, 486 (2006).
- ² K. Y. Bliokh, Y. P. Bliokh, S. Savelev, and F. Nori, *Phys. Rev. Lett.* **99**, 190404 (2007).
- ³ M. Uchida and A. Tonomura, *Nature* **464**, 737 (2010).
- ⁴ B. J. McMorran, A. Agrawal, I. M. Anderson, A. A. Herzog, H. J. Lezec, J. J. McClelland, and J. Unguris, *Science* **331**, 192 (2011).
- ⁵ J. Verbeeck, H. Tian, and P. Schattschneider, *Nature* **467**, 301 (2010).
- ⁶ J. Rusz, J. C. Idrobo, S. Bhowmick, *Phys. Rev. Lett.* **113**, 145501 (2014).
- ⁷ J. Rusz, J. C. Idrobo, *Phys. Rev. B* **93**, 104420 (2016).
- ⁸ J. C. Idrobo, J. Rusz, J. Spiegelberg, M. A. McGuire, C. T. Symons, R. Raju Vatsavai, C. Cantoni, and A. R. Lupini, *Adv. Chem. Struct. Imaging* **2**, 5 (2016).
- ⁹ P.D. McCormack and L. Crane, *Physical Fluid Dynamics*, (Academic Press, New York and London, 1973).
- ¹⁰ J.-Z. Wu, H.-Y. Ma, and M.-D. Zhou, *Vorticity and Vortex Dynamics*, (Springer-Verlag, Berlin Heidelberg, 2006)
- ¹¹ M. V. Berry and M. R. Dennis, *J. Phys. A: Math. Theor.*

40, 65 (2007).

- ¹² P.A.M. Dirac, *The Principles of Quantum Mechanics*, (Clarendon Press, Oxford, 1930).
- ¹³ V. Grillo, E. Karimi, G. C. Gazzadi, S. Frabboni, M. R. Dennis, and R. W. Boyd, *Phys. Rev. X* **4**, 011013 (2014).
- ¹⁴ If spherical aberration C_s is present in the electron microscope, the exponential argument in R_l shown in Eq. 3 can be replaced from $e^{i\frac{\pi}{\lambda}\Delta f\theta^2}$ to $e^{i\frac{\pi}{\lambda}\theta^2(\Delta f + C_s\theta^2/2)}$.
- ¹⁵ R. Shiloh, Y. Tsur, R. Remez, Y. Lereah, B. A. Malomed, V. Shvedov, C. Hnatovsky, W. Krolikowski, and A. Arie, *Phys. Rev. Lett.* **114**, 096102 (2015).
- ¹⁶ O. L. Krivanek, N. Dellby, and M. F. Murfitt, *Aberration Correction in Electron Microscopy*, Handbook of Charged Particle Optics 2nd Edition, edited by Jon Orloff (CRC Press, 2008).
- ¹⁷ A. Lubk, L. Clark, G. Guzzinati, and J. Verbeeck, *Phys. Rev. A* **87**, 033834 (2013).
- ¹⁸ T. C. Petersen, M. Weyland, D. M. Paganin, T. P. Simula, S. A. Eastwood, and M. J. Morgan, *Phys. Rev. Lett.* **110**, 033901 (2013).
- ¹⁹ J. Rusz, S. Bhowmick, M. Eriksson, N. Karlsson, *Phys. Rev. B* **89**, 134428 (2014).

Appendix A: Derivation of the analytical expression for an aberrated beam

Eq. (5), which expresses the analytical form of an aberrated beam can be obtained by analyzing how a plane wave gets diffracted by a circular thin aberrated lens, with an aberration $\chi(\mathbf{k})$. The analytical expression of the diffracted wave ψ by an aberrated lens can be described by

$$\psi(\mathbf{r}) = \int e^{i\mathbf{k}\cdot\mathbf{r}} e^{i\chi(\mathbf{k})} d\mathbf{k}, \quad (\text{A1})$$

where $\mathbf{k} = 2\pi\boldsymbol{\theta}/\lambda$ and \mathbf{r} are the coordinates in the aperture plane and image plane, respectively. For the case of a lens with only one non cylindrical symmetry (besides defocus Δf), the aberrated beam can be expressed as

$$\psi_{n,m}(r, \phi) = \int_0^{2\pi} \int_0^{\theta_c} e^{i\Delta f'\theta^2} e^{ir'\theta \cos(\varphi-\phi)} e^{i\theta^{n+1}C'_{n,m} \cos(m\varphi)} d\varphi d\theta. \quad (\text{A2})$$

To simplify the mathematical notation, here we defined $\Delta f' = \frac{\pi}{\lambda}\Delta f$, $C'_{n,m}$ as $\frac{2\pi}{\lambda(n+1)}C_{n,m,a}$, explicitly omitting the a index for the mirror-symmetric aberration coefficient, and $r' = \frac{2\pi}{\lambda}r$. As it will be shown in a moment, an aberrated beam with an anti-symmetric aberration $C_{n,m,b}$ differs from a mirror-symmetric aberrated beam in a phase coefficient.

Replacing each exponential term in the integral by their respective Jacobi-Anger expansion, Eq. (A2) becomes

$$\psi_{n,m}(r, \phi) = \sum_{l,p=-\infty}^{\infty} i^l i^p e^{-ip\phi} \int_0^{2\pi} e^{i\varphi(p+lm)} d\varphi \int_0^{\theta_c} e^{i\Delta f'\theta^2} J_p(r'\theta) J_l(C'_{n,m}\theta^{n+1}) \theta d\theta, \quad (\text{A3})$$

The integral with respect to φ vanishes unless $p = -lm$. Using the relationship $J_{-l}(x) = (-1)^l J_l(x)$, the diffracted wave $\psi_{n,m}(r, \phi)$ is

$$\psi_{n,m}(r, \phi) = 2\pi \sum_{l=-\infty}^{\infty} i^{-lm} i^l (-1)^{lm} e^{ilm\phi} \int_0^{\theta_c} e^{i\Delta f'\theta^2} J_{lm}(r'\theta) J_l(C'_{n,m}\theta^{n+1}) \theta d\theta, \quad (\text{A4})$$

or written in a more compact form,

$$\psi_{n,m}(r, \phi) = \sum_{l=-\infty}^{\infty} A_{l,m} e^{ilm\phi} P_{l,n,m}(r, \theta_c). \quad (\text{A5})$$

$A_{l,m} = 2\pi i^{l(m+1)}$ is a phase coefficient, and $P_{l,n,m}(r, \theta_c)$ is a radial function resulting from the integral with respect to θ up to a convergence angle θ_c . If the lens instead has only an antisymmetric aberration $C_{n,m,b}$, the diffracted wave $\psi_{n,m}(r, \phi)$ differs from Eq. (A5) only by a new phase coefficient, which can be written as $B_{l,m} = 2\pi i^{lm}$.

Appendix B: Relationship between EMCD and vorticity

DDSCS is given by

$$\frac{\partial^2 \sigma}{\partial \Omega \partial E} \propto \sum_{I,F} \left| \langle \psi_f | \otimes \langle F | \hat{V} | I \rangle \otimes | \psi_i \rangle \right|^2 \delta(E_F - E_I - E) \quad (\text{B1})$$

Writing the real-space incoming-beam wave-function $\psi_i(\mathbf{r})$ via its Fourier components

$$\psi_i(\mathbf{r}) = \int C(\mathbf{k}) e^{i\mathbf{k}\cdot\mathbf{r}} d\mathbf{k} \quad (\text{B2})$$

and approximating the outgoing wave with a plane-wave (point-like detection)

$$\psi_f(\mathbf{r}) = e^{i\mathbf{k}_f \cdot \mathbf{r}} \quad (\text{B3})$$

the DDSCS can be expressed as

$$\frac{\partial^2 \sigma}{\partial \Omega \partial E} \propto \sum_{\mathbf{a}} \iint d\mathbf{k} d\mathbf{k}' C(\mathbf{k}) C^*(\mathbf{k}') e^{i(\mathbf{k}-\mathbf{k}')\cdot\mathbf{a}} \frac{S_{\mathbf{a}}(\mathbf{k}_f - \mathbf{k}, \mathbf{k}_f - \mathbf{k}', E)}{(\mathbf{k}_f - \mathbf{k})^2 (\mathbf{k}_f - \mathbf{k}')^2} \quad (\text{B4})$$

where we introduced MDFFF for atom \mathbf{a} , and a sum over atom positions \mathbf{a} , which originates from the sum over all initial states I .

EMCD signal originates from imaginary parts of the MDFFF, which is in dipole approximation equal to

$$\text{Im}[S_{\mathbf{a}}(\mathbf{q}, \mathbf{q}', E)] \propto (\mathbf{q} \times \mathbf{q}') \cdot \mathbf{M}(E) \quad (\text{B5})$$

with an energy-dependent vector $\mathbf{M}(E)$, which is material-dependent and contains information about spin and orbital magnetism. Furthermore, the factors $C(\mathbf{k})$ can be written via inverse Fourier transform of the incoming beam

$$C(\mathbf{k}) = \int \psi_i(\mathbf{r}) e^{-i\mathbf{k}\cdot\mathbf{r}} d\mathbf{r} \quad (\text{B6})$$

Using these expressions we can write the DDSCS as

$$\frac{\partial^2 \sigma}{\partial \Omega \partial E} \propto \sum_{\mathbf{a}} \iiint d\mathbf{r} d\mathbf{r}' d\mathbf{k} d\mathbf{k}' \psi_i(\mathbf{r}) e^{-i\mathbf{k}\cdot\mathbf{r}} \psi_i^*(\mathbf{r}') e^{i\mathbf{k}'\cdot\mathbf{r}'} e^{i(\mathbf{k}-\mathbf{k}')\cdot\mathbf{a}} \frac{i(\mathbf{k}_f - \mathbf{k}) \times (\mathbf{k}_f - \mathbf{k}')}{(\mathbf{k}_f - \mathbf{k})^2 (\mathbf{k}_f - \mathbf{k}')^2} \cdot \mathbf{M}(E) \quad (\text{B7})$$

We choose a coordinate system, in which $\mathbf{k}_f \parallel z$ -axis. Then the MDFFF part can be written as

$$\frac{i(\mathbf{k}_f - \mathbf{k}) \times (\mathbf{k}_f - \mathbf{k}')}{(\mathbf{k}_f - \mathbf{k})^2 (\mathbf{k}_f - \mathbf{k}')^2} \cdot \mathbf{M}(E) = i\mathbf{M}(E) \cdot \frac{\mathbf{k} \times \mathbf{k}' + \mathbf{k}_f \times (\mathbf{k} - \mathbf{k}')}{[k_{\perp}^2 + (k_f - k_z)^2][k'_{\perp}{}^2 + (k'_f - k'_z)^2]} \quad (\text{B8})$$

Now we note that for an incoming beam wavefunction that vanishes in infinity, under an integral we can write

$$\int i\mathbf{k} \psi_i(\mathbf{r}) e^{i\mathbf{k}\cdot\mathbf{r}} d\mathbf{r} = \int \nabla \psi_i(\mathbf{r}) e^{i\mathbf{k}\cdot\mathbf{r}} d\mathbf{r} \quad (\text{B9})$$

using the theorem about Fourier transform of a derivative of a function.

This allows us to rewrite the entire DDSCS as a sum of two terms

$$\begin{aligned} \frac{\partial^2 \sigma}{\partial \Omega \partial E} &\propto i\mathbf{M}(E) \cdot \sum_{\mathbf{a}} \iiint d\mathbf{r} d\mathbf{r}' d\mathbf{k} d\mathbf{k}' \frac{e^{-i\mathbf{k}\cdot(\mathbf{r}-\mathbf{a})}}{k_{\perp}^2 + (k_f - k_z)^2} \frac{e^{i\mathbf{k}'\cdot(\mathbf{r}'-\mathbf{a})}}{k'_{\perp}{}^2 + (k_f - k'_z)^2} \\ &\times [\nabla\psi_i(\mathbf{r}) \times \nabla'\psi_i^*(\mathbf{r}') + \mathbf{k}_f \times (\nabla - \nabla')\psi_i(\mathbf{r})\psi_i^*(\mathbf{r}')] \end{aligned} \quad (\text{B10})$$

where ∇' means a gradient in the primed index \mathbf{r}' . The first term formally reminds vorticity, but it is evaluated at two independent coordinates. Nevertheless, we will deal with integrals over \mathbf{k}, \mathbf{k}' first.

We need to evaluate

$$\int \frac{e^{-i\mathbf{k}\cdot(\mathbf{r}-\mathbf{a})}}{k_{\perp}^2 + (k_f - k_z)^2} d\mathbf{k} = \int_{-\infty}^{\infty} dk_z \int_0^{2\pi} d\phi \int_0^{\infty} k_{\perp} dk_{\perp} \frac{e^{-ik_z z} e^{-ik_{\perp} x_{\perp} \cos \phi}}{k_{\perp}^2 + (k_f - k_z)^2} \quad (\text{B11})$$

where $z = r_z - a_z$ and $x_{\perp} = \sqrt{(r_x - a_x)^2 + (r_y - a_y)^2}$.

For the integral over ϕ we can use Jacobi-Anger identity

$$e^{iz \cos \phi} = \sum_{n=-\infty}^{\infty} i^n J_n(z) e^{in\phi} \quad (\text{B12})$$

from which only the term $n = 0$ survives, giving

$$2\pi \int_{-\infty}^{\infty} dk_z e^{-ik_z z} \int_0^{\infty} k_{\perp} dk_{\perp} \frac{J_0(k_{\perp} x_{\perp})}{k_{\perp}^2 + (k_f - k_z)^2} \quad (\text{B13})$$

The integral over k_{\perp} gives a modified Bessel function of the second kind

$$2\pi \int_{-\infty}^{\infty} dk_z e^{-ik_z z} K_0(x_{\perp} |k_f - k_z|) \quad (\text{B14})$$

This can be written as

$$2\pi e^{-ik_f z} \int_{-\infty}^{\infty} dk_z e^{-i(k_z - k_f)z} K_0(x_{\perp} |k_z - k_f|) = 2\pi e^{-ik_f z} \int_{-\infty}^{\infty} d\tilde{k} e^{-i\tilde{k}z} K_0(x_{\perp} |\tilde{k}|) \quad (\text{B15})$$

and split to two integrals from $-\infty$ to 0 and from 0 to ∞ , which are complex conjugates of each other, i.e., the entire integral becomes

$$4\pi e^{-ik_f z} \int_0^{\infty} \cos(\tilde{k}z) K_0(x_{\perp} \tilde{k}) d\tilde{k} = 4\pi e^{-ik_f z} \frac{1}{x_{\perp}} \frac{\pi}{2\sqrt{\left(\frac{z}{x_{\perp}}\right)^2 + 1}} = \frac{2\pi^2 e^{-ik_f(r_z - a_z)}}{|\mathbf{r} - \mathbf{a}|} \quad (\text{B16})$$

which we can write in a coordinate-independent form as

$$\frac{2\pi^2 e^{-i\mathbf{k}_f \cdot (\mathbf{r} - \mathbf{a})}}{|\mathbf{r} - \mathbf{a}|} \quad (\text{B17})$$

Now we return to the DDSCS. Integrals over \mathbf{k}, \mathbf{k}' are evaluated, so we have

$$\begin{aligned} \frac{\partial^2 \sigma}{\partial \Omega \partial E} &\propto 4\pi^4 i\mathbf{M}(E) \cdot \sum_{\mathbf{a}} \iint d\mathbf{r} d\mathbf{r}' \frac{e^{-i\mathbf{k}_f \cdot (\mathbf{r} - \mathbf{r}')}}{|\mathbf{r} - \mathbf{a}| |\mathbf{r}' - \mathbf{a}|} \\ &\times [\nabla\psi_i(\mathbf{r}) \times \nabla'\psi_i^*(\mathbf{r}') + \mathbf{k}_f \times (\nabla - \nabla')\psi_i(\mathbf{r})\psi_i^*(\mathbf{r}')] \end{aligned} \quad (\text{B18})$$

Qualitatively it is obvious that the largest weight in front of the vorticity-like expression (2nd line) comes from the nearest surrounding of the points $\mathbf{r} = \mathbf{r}' = \mathbf{a}$, which means that the magnetic signal should be approximately proportional to the sum of the electron beam vorticities projected on the magnetization direction (often the optical axis).

Further insight can be obtained by expressing the incoming wavefunction in an Ansatz commonly used in multislice methods, i.e., plane-wave along incoming beam direction times a relatively smooth envelope function

$$\psi_i(\mathbf{r}) = e^{i\mathbf{k}_i \cdot \mathbf{r}} \phi_i(\mathbf{r}) \quad (\text{B19})$$

gradient of which is

$$\nabla\psi_i(\mathbf{r}) = e^{i\mathbf{k}_i\cdot\mathbf{r}}(i\mathbf{k}_i + \nabla)\phi_i(\mathbf{r}) \quad (\text{B20})$$

Then the first term becomes

$$\nabla\psi_i(\mathbf{r}) \times \nabla'\psi_i^*(\mathbf{r}') = e^{i\mathbf{k}_i\cdot(\mathbf{r}-\mathbf{r}')} [i\mathbf{k}_i \times (\nabla + \nabla') + \nabla \times \nabla'] \phi_i(\mathbf{r}) \phi_i^*(\mathbf{r}') \quad (\text{B21})$$

and the second term

$$\mathbf{k}_f \times (\nabla - \nabla')\psi_i(\mathbf{r})\psi_i^*(\mathbf{r}') = e^{i\mathbf{k}_i\cdot(\mathbf{r}-\mathbf{r}')} \mathbf{k}_f \times [2i\mathbf{k}_i + (\nabla - \nabla')] \phi_i(\mathbf{r}) \phi_i^*(\mathbf{r}') \quad (\text{B22})$$

Therefore, in a common situation when $\mathbf{k}_i \parallel \mathbf{M}(E)$, the magnetic part of the DDSCS reduces to

$$\begin{aligned} \frac{\partial^2 \sigma}{\partial \Omega \partial E} &\propto 4\pi^4 i \mathbf{M}(E) \cdot \sum_{\mathbf{a}} \iint d\mathbf{r} d\mathbf{r}' \frac{e^{-i(\mathbf{k}_f - \mathbf{k}_i) \cdot (\mathbf{r} - \mathbf{r}')}}{|\mathbf{r} - \mathbf{a}| |\mathbf{r}' - \mathbf{a}|} \\ &\quad \times [\nabla\phi_i(\mathbf{r}) \times \nabla'\phi_i^*(\mathbf{r}') + \mathbf{k}_f \times (\nabla - \nabla')\phi_i(\mathbf{r})\phi_i^*(\mathbf{r}')] \end{aligned} \quad (\text{B23})$$

where we identify $\mathbf{Q} = \mathbf{k}_f - \mathbf{k}_i$ as the momentum transfer vector. If also $\mathbf{k}_f \parallel \mathbf{M}(E)$, then the last term drops as well. Alternatively, an integral over \mathbf{k}_f spanning a symmetrical on-axis detector leads to a vanishing z -component of $\mathbf{k}_f \times (\nabla - \nabla')\phi_i(\mathbf{r})\phi_i^*(\mathbf{r}')$, therefore the last term drops in such situation as well. This can be shown by summation over pairs of \mathbf{k}_f , where $\mathbf{k}_f = (k_x, k_y, k_z)$ and its paired $\mathbf{k}'_f = (-k_x, -k_y, k_z)$. Then $\mathbf{k}_f + \mathbf{k}'_f = (0, 0, 2k_z)$ and its vector product with anything must be perpendicular to z -direction.

Thus, for the magnetization along the optical axis and on-axis detection the magnetic signal is determined by an expression containing a non-local form of a vorticity-like expression

$$\frac{\partial^2 \sigma}{\partial \Omega \partial E} \propto 4\pi^4 i \sum_{\mathbf{a}} \iint d\mathbf{r} d\mathbf{r}' \frac{e^{-i(\mathbf{k}_f - \mathbf{k}_i) \cdot (\mathbf{r} - \mathbf{r}')}}{|\mathbf{r} - \mathbf{a}| |\mathbf{r}' - \mathbf{a}|} [\nabla\phi_i(\mathbf{r}) \times \nabla'\phi_i^*(\mathbf{r}')] \cdot \mathbf{M}(E) \quad (\text{B24})$$

from which follows the Eq. (13) in the main text of the document, where an integration over \mathbf{k}_f over a symmetric on-axis detector was assumed.